UNITED STATES
DEPARTMENT OF THE INTERIOR
GEOLOGICAL SURVEY

National Center for Earthquake Research
345 Middlefield Road
Menlo Park, California 94025

PREDICTION OF MAXIMUM EARTHQUAKE INTENSITIES FOR THE SAN FRANCISCO BAY REGION

by

Roger D. Borcherdt and James F. Gibbs

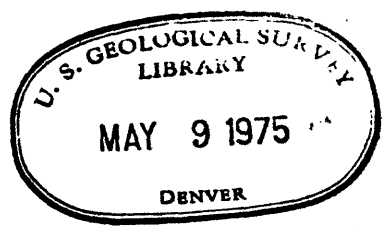

Open-File Report 75-180
1975

PREDICTION OF MAXIMUM EARTHQUAKE INTENSITIES FOR THE SAN FRANCISCO BAY REGION

by

Roger D. Borcherdt and James F. Gibbs

ABSTRACT

The intensity data for the California earthquake of April 18, 1906, are strongly dependent on distance from the zone of surface faulting and the geological character of the ground. Considering only those sites (approximately one square city block in size) for which there is good evidence for the degree of ascribed intensity, the empirical relation derived between 1906 intensities and distance perpendicular to the fault for 917 sites underlain by rocks of the Franciscan Formation is

$$\text{Intensity} = 2.69 - 1.90 \log (\text{Distance}) \text{ (km)}.$$

For sites on other geologic units intensity increments, derived with respect to this empirical relation, correlate strongly with the Average Horizontal Spectral Amplifications (AHSA) determined from 99 three-component recordings of ground motion generated by nuclear explosions in Nevada. The resulting empirical relation is

$$\text{Intensity Increment} = 0.27 + 2.70 \log (\text{AHSA}),$$

and average intensity increments for the various geologic units are -0.29 for granite, 0.19 for Franciscan Formation, 0.64 for the Great Valley Sequence, 0.82 for Santa Clara Formation, 1.34 for alluvium, 2.43 for bay mud. The maximum intensity map predicted from these empirical relations delineates areas in the San Francisco Bay region of potentially high intensity from future earthquakes on either the San Andreas fault or the Hayward fault.

INTRODUCTION

The amounts of damage resulting from the great California earthquake of April 18, 1906, varied greatly for different areas in the San Francisco Bay region. In some areas the damage was WEAK with "occasional fall of chimneys and damage to plaster, partitions, plumbing and the like," in other nearby areas the damage was VIOLENT with "...fairly general collapse of brick and frame structures when not unusually strong ..." (Wood, 1908). These large variations were due in part to distance from the zone of surface faulting and in part to the geological character of the ground (compare the intensity map for the city of San Francisco (fig. 1) with the geologic map (fig. 2)). The purposes of this paper are to first quantify the dependencies of the 1906 intensities on distance and the geological character of the ground; then, second, to use the resulting empirical relationships to predict maximum intensities at a scale of 1:125,000 for the San Francisco Bay region from possible future earthquakes.

The earthquake vulnerability of the San Francisco Bay region defines a strong need to anticipate the effects of future large earthquakes likely to occur on the San Andreas and Hayward faults. Earthquake intensities predicted on a standardized map base at a scale of 1:125,000 are useful for anticipating such effects in a general qualitative way at specific sites and for delineating geographically earthquake problem areas. Such predictions are especially needed for a large earthquake on the Hayward fault as there is little prior intensity data available for such an earthquake. In addition, predictions are needed for a large earthquake on the San Andreas fault in areas not developed at the time of the 1906 earthquake.

The quality of the evidence for the intensities ascribed following the 1906 earthquake varied greatly. In some areas, for example, downtown San Francisco, the density of structures was sufficient to provide redundant evidence for the degree of ascribed intensity and to permit detailed delineations of variations in intensity levels. In other less densely populated areas, intensities were ascribed on the basis of evidence observed at sites kilometers apart with resulting lack of detail in the delineations of ascribed intensity.

In the following analyses only the intensity data from those sites (approximately one square city block in size) for which there was good evidence were utilized. In the city of San Francisco (Map no. 19, Lawson, 1908), only those sites defined by Wood (1908) as having "unequivocal" evidence were considered. For the southern San Francisco peninsula (Maps nos. 21 and 22, Lawson, 1908), only those sites intersected by an examined route were considered.

Utilization of only the good 1906 intensity data, detailed geologic mapping, and the comparative ground motion measurements for 99 sites permit predictions of intensities in considerably more detail for some areas than it was possible to ascribe following the 1906 earthquake.

Two previous maps of predicted intensity have been prepared for the San Francisco Bay region (Algermissen and others, 1972; Evernden and others, 1973). The map by Algermissen and others (1972) was prepared at a scale of 1 cm $\approx$ 7 km and is based on nonexplicit relations between intensity, distance, and site geology. Evernden and others (1973) prepared a map of predicted intensity for central California at a scale of 1 cm $\approx$ 1.3 km and a map for the city of San Francisco at a scale of 1 cm $\approx$ 1 km. These maps were constructed from a numerical model of the earthquake source which estimated relative peak acceleration values for a standard ground condition at various distances from the potential earthquake source, with these acceleration values (a) being converted to intensity values (I) using the empirical relation

$$I = 3(0.5 + \log a).$$

Their map of predicted intensities was then obtained by convolving the map for uniform ground conditions with a map on which the actual geological ground conditions were characterized by relative intensity values determined from data of Borcherdt (1970). Their numerical model was calibrated according to selected sites with good 1906 intensity data (see Evernden and others, 1973, for details). This study differs from the preceding in that the predictions are based on explicit relations, derived for this study, between the good 1906 intensity data, distance, and the geological character of the ground. In addition, the predictions from this study require no assumptions as to numerical models of the earthquake source or relationships of peak acceleration to intensity, they are presented at a scale of 1:125,000 (1 cm $\approx$ 1.25 km) on a standardized map base which permits identification of streets and other cultural features, and they are based on a generalized geologic map recently compiled at the same scale by Lajoie (personal commun., 1974).

INTENSITY VS. DISTANCE

The 1906 earthquake intensities ascribed sites on the same geologic unit generally decrease with increasing distance from the zone of surface faulting (Lawson, 1908). To quantify this apparent relationship the 1906 intensity data for the San Francisco Bay region were reconsidered on a site-by-site basis. The intensity data from only those sites (approximately one square city block in size) for which was good evidence for the degree of ascribed intensity were considered. For each site underlain by rocks of the Franciscan Formation the perpendicular distance to the zone of 1906 surface faulting was measured and plotted as a function of the ascribed 1906 earthquake intensity (fig. 3). The resulting empirical relation,

$$\text{Intensity} = 2.69 - 1.90 \log (\text{Distance (km)}),$$

determined by the method of least squares over the distance interval 0-15 km suggests that the ascribed intensity values for sites on the Franciscan Formation generally decrease as the logarithm of increasing distance. The empirical relation shows that the intensity values decrease very rapidly with distance, with sites 3 km from the fault having observed intensities more than two intensity units smaller than those at the fault.

The sites with the highest ascribed intensities ("A", 1906 San Francisco scale) are located within 0.7 km of the center of the zone of surface rupture. For most of these sites the unit of intensity was assigned on the basis of evidence for some form of ground failure most of which was associated with surface faulting. The degree of intensity assigned to most of the other sites at greater distances from the fault was based on damage resulting from ground shaking or ground shaking induced ground failures. To quantify the dependence of the intensities due only to shaking on distance, another empirical relation was determined with the intensity data near the fault omitted. The resulting empirical relation Intensity = 2.71 - 1.96 log (Distance (km)) is essentially the same as the one determined from the complete data set. (Intensities predicted by either relation differ by 0.09 at distances less than 0.16 km and less than 0.05 for distances in the interval 0.8 to 15 km). This similarity suggests that the dependence of intensity on distance is not influenced by the intensity data near the fault due to surface faulting. For explicitness only the relation determined from the complete data set will be referred to hereafter. The means and standard deviations for the samples are tabulated (table 1). The standard error of the regression coefficients for the restricted and complete data sets are 0.04 and 0.03, respectively.

INTENSITY INCREMENT VS. LOW-STRAIN AMPLIFICATION

Three components of ground motion generated by distant nuclear explosions in Nevada have been recorded at 99 sites in the San Francisco Bay region (Borcherdt, 1970; Gibbs and Borcherdt, 1974).

Analysis of these recordings shows that certain frequencies of the low-strain ground motions are amplified considerably by certain types of local site conditions. Borcherdt (1970) showed that spectral amplification curves computed with respect to a given bedrock unit to a first approximation isolate the seismic response characteristics of the local site conditions. To isolate the dependence of the observed 1906 intensities on local site conditions (from the dependence of the intensities on distance), intensity increments were defined for each of the recording sites for which 1906 intensity data are available. The intensity increment for each site was defined as the difference between the observed intensity and the intensity predicted by the empirical relation for sites at the same distance on the Franciscan Formation (fig. 3).

The intensity increments are plotted as a function of the Average Horizontal Spectral Amplification (AHSA) values computed with respect to the Franciscan Formation from the low-strain ground motion recordings (fig. 4). Empirical relations were determined using the method of least squares from only the data ("•") for sites in the city of San Francisco for which there was "unequivocal evidence" for the degree of ascribed 1906 intensity and from the complete data set ("." and "•"). The two empirical relations are similar with intensity increments predicted by either relation differing by less than two-tenths (see fig. 3). The empirical relation ($\delta I = 0.27 + 2.70 \log (AHSA)$) based on only the good intensity data in the city of San Francisco is preferred. The means and standard deviations for the samples are tabulated (table 1). The standard error of the regression coefficient for the restricted data set is 0.29 and for the complete data set is 0.33.

The correlation coefficient of 0.95 computed for the preferred empirical relation ($\delta I = .27 + 2.70 \log (AHSA)$) shows that a strong correlation exists between the computed intensity increments and the amplifications observed at low-strain levels. The physical meaning of this empirical correlation is complex and does not necessarily mean that amplifications observed at low-strain levels can be extrapolated directly to high-strain levels. However, there are two possible reasons for this correlation:

(1) For levels of ground shaking that did not cause ground failure, the higher amplifications indicate those sites that experienced the higher levels of ground shaking, and

(2) For levels of ground shaking that did induce ground failure, the higher amplifications indicate those sites that were most susceptible to ground failure.

In either case, the higher amplifications indicate those sites that experienced greater amounts of damage and, hence, were assigned higher degrees of intensity.

PREDICTION OF MAXIMUM EARTHQUAKE INTENSITIES AT LOW-STRAIN RECORDING SITES

Historically large earthquakes have occurred along both the San Andreas and Hayward faults. Recent fault studies (e.g., Wesson and others, 1974) indicate a high potential exists for future large earthquakes (magnitude, 7.6-8.3) along both faults. As the types of faulting and maximum potential earthquake intensities are similar for the San Andreas and Hayward faults, the 1906 intensity attenuation curve (fig. 3) may be considered useful for intensity predictions for a large earthquake on the Hayward fault as well as one on the San Andreas fault. Such predictions from the 1906 intensity attenuation curve are valid for sites on the Franciscan Formation. For sites not on the Franciscan Formation, the empirical relation between intensity increment and the low-strain amplification permits an appropriate correction to the predicted intensity. Hence, for each of the sites with measured low-strain amplifications intensities can be predicted from the two empirical curves for a large earthquake on either fault. Such predictions require only the geologic information needed to delineate the Franciscan Formation as opposed to that needed to delineate the other goelogic units.

Intensities are predicted for each of the sites at which amplifications have been measured (table 1). The maximum of the intensities predicted for large earthquakes on the San Andreas fault and on the Hayward fault is plotted (fig. 6). The map suggests that a future earthquake on either of the faults could cause as much damage at sites some distance from the faults as at sites in the immediate zones of potential surface faulting. Also, the map suggests that the earthquake hazard is not uniformly distributed throughout the San Francisco Bay region and that large variations in damage might be expected over relatively short distances.

To compare the predicted intensities for an earthquake on the San Andreas with the observed 1906 intensities (table 1, cols. 8 and 9), two types of recording sites were considered. Those sites with ascribed 1906 intensities regardless of the quality of evidence were considered as one sample and those with intensities ascribed on the basis of "unequivocal" evidence were considered as another sample. (The intensity values predicted from the empirical relations based on only the good intensity data are plotted as a function of the observed values (fig. 5).) The mean and standard deviation of the difference between the predicted and observed values for the sites with "unequivocal" evidence are 0.03 and 0.39, respectively, and for all of the sites they are 0.06 and 0.73, respectively. The mean and standard deviation for the absolute value of the difference between the predicted and observed values are 0.29 and 0.24, respectively, for the "unequivocal" data and 0.58 and 0.43, respectively, for all the data. The larger values for the sample including all of the data are consistent with the fact that the quality of the intensity evidence is less for this sample. The mean value of 0.29 and the standard deviation 0.24 may be interpreted as indicative of the uncertainty associated with the predicted intensity values at the sites for which low-strain amplifications have been measured.

The maximum earthquake intensities (fig. 6) are predicted for the large number of sites at which low-strain amplifications have been measured and these predictions could be used to draw contours of equal intensity for the entire area. However, a better approach for predicting intensities continuously throughout the region is one based on the available detailed geologic mapping.

INTENSITY INCREMENTS VS. LOCAL GEOLOGIC UNITS

The amounts of damage from numerous past earthquakes have been observed to depend strongly on the geological character of the ground (see Duke, 1958, for a comprehensive bibliography). To investigate this dependence for the 1906 earthquake, the measured intensity increments computed at each of the recording sites are grouped according to the type of underlying geologic unit (table 1, col. 5) (see appendix 2 for descriptions of geologic units).

The measured intensity increments establish that a strong correlation exists between the observed 1906 intensities and the type of geologic unit. The mean intensity increments increase with decreasing "firmness" of the geologic units showing that in general the greatest amounts of damage, excluding that in the immediate zone of surface faulting, occurred on the softest sites. These sites are in general susceptible to the largest amount of ground shaking amplification (Borcherdt, 1970) and to the greatest amounts of liquefaction induced ground failures (Youd, 1974).

The means for the samples of measured intensity increments computed for the various geologic units (table 1, col. 5) were based on the intensity data from all of the recording sites regardless of the quality of evidence. In the authors' opinion, an improved quantification of the intensity dependence on the geologic unit is obtained by considering the intensity increments predicted at each of the recording sites using the empirical intensity increment vs. amplification curve (fig. 4), which is based on only that intensity data for which there was unequivocal evidence. The intensity increments predicted from this curve are tabulated (table 1, col. 6), and grouped according to the type of geologic unit. The means and standard deviations for the various samples are shown at the bottom of each tabulation for the corresponding geologic unit in table 1, cols. 5 and 6. These means and standard deviations were computed for all of the sites in each sample, including those for which it was necessary to predict the intensity increments from the analog amplifications. The means and standard deviations for the sites in each sample for which the intensity increments were predicted from the spectral amplifications are summarized in table 2. These means (table 2) are preferred as a quantitative estimate of the dependence of the 1906 earthquake intensities on the geological character of the ground.

PREDICTION OF MAXIMUM EARTHQUAKE INTENSITIES ON A REGIONAL BASIS

The lack of prior intensity data for many areas in the San Francisco Bay region and the high earthquake vulnerability of the region define a definite need for intensity predictions on a regional basis. To make regional predictions a generalized geologic map was compiled at a scale of 1:125,000 by Lajoie (personal commun., 1974). The map delineates the geologic units determined to have significantly different seismic responses (Gibbs and Borcherdt, 1974).

Utilizing the mean intensity increments for the generalized geologic units predicted on the basis of the good 1906 intensity data (table 2), the empirical intensity vs. distance relation (fig. 3), and the generalized geologic map, intensities were predicted on a regional basis (fig. 7). Areas are delineated on the map (fig. 7) according to the various grades of predicted intensity defined by the San Francisco intensity scale. Use of the San Francisco scale reduces uncertainties in the predictions that would result from conversion to another intensity scale which requires consideration of intensity data from other areas. Comparisons between the Rossi-Forel scale, the San Francisco scale, and the modified Mercalli scale as presented by Wood (1908), Wood and Newmann (1931), and Richter (1958), are presented in figure 8. Some of the boundaries separating various grades of intensity on the map (fig. 7) coincide with geologic boundaries and the others were dictated on the basis of distance corresponding to the appropriate geologic unit. The intensity shown for each area is the maximum of that assuming large earthquakes on the San Andreas and Hayward faults. The standard deviations computed for the samples of predicted intensity increments associated with the various geologic units (table 2) are indicative of the variability associated with the predictions.

The map predicts zones of "very violent" ("A") intensity for linear zones along the faults and for areas relatively close to the faults underlain by younger bay mud. The widths of the "very violent" zones along the faults vary depending on the type of neighboring geologic unit. The widest zones occur in areas along the faults underlain by older bay sediments.

The predicted intensity map shows more detailed geographic delineations of intensity in some areas than does the 1906 intensity map. This is especially true for areas south of the city of San Francisco (Maps nos. 21 and 22, Lawson, 1908). The more detailed delineations are due to the detailed geologic control currently available and the scarcity of 1906 intensity data available in some areas. The map delineates earthquake problem areas and shows, as did the 1906 intensity maps, that earthquake hazards are not uniformly distributed throughout the San Francisco Bay region.

CONCLUSIONS

The apparent dependencies of the 1906 earthquake intensities on the geological character of the ground and distance from the zone of surface faulting have been quantified using only the good 1906 intensity data.

The empirical relation derived between intensity and perpendicular distance to the fault for 917 sites (approximately one square city block in size) on the Franciscan Formation is

$$\text{Intensity} = 2.69 - 1.90 \log (\text{Distance (km)}).$$

Omission of the intensity data due to surface faulting did not influence this intensity vs. distance relationship. Intensity increments between the observed intensity and that predicted by this derived distance relation correlate strongly with the measured low-strain amplifications of ground motion generated by nuclear explosions in Nevada. The empirical relation derived between the low-strain amplifications and the intensity increments is

$$\text{Intensity Increment} = 0.27 + 2.70 \log (\text{AHSA}).$$

This empirical relation was derived from the data at the 11 recording sites for which "unequivocal" evidence exists for the degree of ascribed 1906 intensity. The intensities predicted for the remaining 88 recording sites on the basis of the two preceding empirical relations provide estimates of the intensity that might result from future large earthquakes on either the San Andreas or Hayward faults.

The predicted intensity values for a future large earthquake on the San Andreas fault show good agreement with those actually ascribed following the 1906 earthquake. The means and standard deviations for the magnitude difference between the predicted and observed intensity values for 46 sites are 0.58 and 0.43, respectively. The intensities predicted at the low strain recording sites were derived independent of any geologic data in addition to that on the Franciscan Formation and they suggest that many sites with no prior intensity data may be sites of high intensity in future large earthquakes.

The average intensity increments derived for various geologic units provided a quantitative estimate of the dependence of the 1906 intensities on the geological character of the ground. The means and standard deviations derived for the various geologic units are summarized in table 2.

The maximum earthquake intensities predicted on a regional basis using the generalized geologic map compiled at a scale of 1:125,000 help delineate general earthquake problem areas in the San Francisco Bay region. Numerous earthquake problem areas--in addition to those defined by the 1906 earthquake--are delineated on the map (fig. 7).

REFERENCES

Algermissen, S. T. (principal investigator), 1972, A study of the earthquake losses in the San Francisco Bay Area: NOAA report, 220 p.

Borcherdt, R. D., 1970, Effects of local geology on ground motion near San Francisco Bay: Seismol. Soc. America Bull., v. 60, p. 29-61.

Duke, C. M. (compiler), 1958, Bibliography of effects of soil conditions on earthquake damage: Earthquake Eng. Inst. 47.

Evernden, J. F., Hibbard, R. R., and Schneider, J. F., 1973, Interpretation of seismic intensity data: Seismol. Soc. America Bull., v. 63, p. 399-422.

Gibbs, J. F., and Borcherdt, R. D., 1974, Effects of local geology on ground motion in the San Francisco Bay region--a continued study: U.S. Geol. Survey open-file report 74-222.

Gibbs, J. F., and Eaton, J. P., 1971, A digitized map of seismic ground response of the San Francisco Bay region, California: U.S. Geol. Survey open-file map.

Lawson, A. C. (chairman), 1908, The California earthquake of April 18, 1906, Report of the State Earthquake Commission: Carnegie Inst. Washington Pub. 87, Washington, D.C.

Richter, C. F., 1958, Elementary seismology: W. H. Freeman and Co., San Francisco, Calif., 768 p.

Schlocker, J., Bonilla, M. G., and Radbruch, D. H., 1958, Geology of the San Francisco north quadrangle, California: U.S. Geol. Survey Misc. Geol. Inv. Map I-272.

Wesson, R. L., Wentworth, C. M., Brown, R. D., Jr., Helley, E. J., and Lajoie, K. R., 1975, Faults and future earthquakes, in Studies for seismic zonation of the San Francisco Bay region: U.S. Geol. Survey Prof. Paper 934A.

Wood, H. O., 1908, Distribution of apparent intensity in San Francisco, in The California earthquake of April 18, 1906, Report of the State Earthquake Investigation Commission: Carnegie Inst. Washington Pub. 87, Washington, D.C., p. 220-245.

Wood, H. O., and Newmann, F., 1931, Modified Mercalli intensity scale of 1931: Seismol. Soc. America Bull., v. 53, p. 979-987.

Youd, T. L., Nichols, D. R., Helley, E. J., and Lajoie, K. R., 1975, Liquefaction potential, in Studies for seismic zonation of the San Francisco Bay region: U.S. Geol. Survey Prof. Paper 934A.

APPENDIX 1

The following grades of apparent intensity were ascribed by H. O. Wood (1908, p. 224-225) in the city of San Francisco after the California earthquake of April 18, 1906.

Grade A. Very violent - Comprizes the rending and shearing of rock masses, earth, turf, and all structures along the line of faulting; the fall of rock from mountain sides; numerous landslips of great magnitude; consistent, deep, and extended fissuring in natural earth; some structures totally destroyed.

Grade B. Violent - Comprizes fairly general collapse of brick and frame buildings when not unusually strong; serious cracking of brick work and masonry in excellent structures; the formation of fissures, step faults, sharp compression anticlines, and broad, wave-like folds in paved and asphalt-coated streets, accompanied by the ragged fissuring of asphalt; the destruction of foundation walls and underpinning structures by the undulation of the ground; the breaking of sewers and water-mains; the lateral displacement of streets; and the compression, distension, and lateral waving or displacement of well-ballasted street-car tracks.

Grade C. Very strong - Comprizes brick work and masonry badly cracked, with occasional collapse; some brick and masonry gables thrown down; frame buildings lurched or listed on fair or weak underpinning structures, with occasional falling from underpinning or collapse; general destruction of chimneys

and of masonry, brick or cement veneers; considerable cracking or crushing of foundation walls.

Grade D. Strong - Comprizes general but not universal fall of chimneys; cracks in masonry and brick work; cracks in foundation walls, retaining walls, and curbing; a few isolated cases of lurching or listing of frame buildings built upon weak underpinning structures.

Grade E. Weak - Comprizes occasional fall of chimneys and damage to plaster, partitions, plumbing, and the like.

APPENDIX 2

(1) Bay mud (equivalent to the younger bay mud unit referred to by Borcherdt (1970)) consists mostly of recently-deposited, plastic, organic-rich, soft clay, silt and minor sand with more than 50 weight percent water; thicknesses up to 40 m (130 ft) and shear velocities 90 to 130 m/sec (290 to 430 ft/sec).

(2) Alluvium (equivalent to the older bay sediment unit referred to by Borcherdt (1970)) comprises the Holocene and Late Pleistocene alluvial units which consist mostly of silty sandy clay, silty clayey sand, and sand and gravel with less than 40 weight percent water; thicknesses up to 600 m (2,000 ft), and shear velocities approximately 200 m/sec (640 ft/sec) at the surface increasing with depth.

(3) Bedrock comprises Pliocene and Early Pleistocene deposits which include the Santa Clara and Merced Formations, consisting of semi-indurated and indurated sandstone, siltstone, and mudstone; Tertiary rocks, consisting of marine sandstone and shale of Eocene, Miocene, and Pliocene age, Page Mill Basalt, lava flows, and pyroclastics of Miocene age; and pre-Tertiary rocks, which include the Franciscan Formation, consisting mostly of sandstone, shale, radiolarian chert, and greenstone (volcanic rocks), minor amounts of granitic rocks, and the Great Valley sequence, consisting of indurated sandstones and siltstones; varying thicknesses, and shear velocities estimated to range from 500 to 2,000m/sec (1,600-6,500 ft/sec).

FIGURE CAPTIONS

Figure 1. Map showing distribution of apparent intensities of the 1906 earthquake in the city of San Francisco, California (San Francisco scale, see appendix 1 for detailed description) (after Wood, 1908).

Figure 2. Map showing distribution of geologic units for the city of San Francisco, California (compiled by K. R. Lajoie from data of Schlocker and others, 1958).

Figure 3. Observed 1906 intensities for sites (one square city block in size) underlain by rocks of the Franciscan Formation versus perpendicular distance from the zone of surface rupture during the 1906 earthquake. For sites with "unequivocal evidence" in the city of San Francisco (Map no. 19, Lawson, 1908), the number of observed intensity values is shown below the corresponding distance interval. For sites intersected by an "examined route" south of the city of San Francisco (Maps nos. 21 and 22, 1908), the number of observed intensities is shown above the corresponding distance interval. The observed 1906 intensities are expressed in terms of the 1906 San Francisco intensity scale with the letters A-E corresponding respectively to the numbers 4-0 (see appendix 1 for detailed description of intensity scale).

Figure 4. Increments in 1906 intensities versus average horizontal spectral amplification computed at corresponding sites from recordings of nuclear explosions. Both the intensity increment values and the average horizontal spectral amplification values were computed with respect to the corresponding average value determined for sites underlain by rocks of the Franciscan Formation. The empirical relation ($\delta I = 0.19 + 2.97 \log(AHSA)$) is based on the data (".") from all of the recording sites for which there was an observed 1906 intensity value. The empirical relation ($\delta I = 0.27 + 2.70 \log(AHSA)$) is based on only the data ("•") from sites in the city of San Francisco for which there was unequivocal evidence for the degree of ascribed 1906 intensity.

Figure 5. Observed 1906 intensity values for the low-strain recording sites versus the intensity values for an earthquake on the San Andreas predicted on the basis of the empirical relations derived from only the good 1906 intensity data (empirical relations shown in figs. 3 and 4). The line shown with zero intercept and unit slope provides a base line for comparing the observed and predicted values (numbers 4-0 correspond to letters A-E respectively of San Francisco intensity scale).

Figure 6. Predicted maximum earthquake intensities for low-strain recording sites based on empirical relations derived from only good 1906 intensity data (see text) (numbers 4-0 correspond to letters A-E respectively of San Francisco intensity scale). The predicted intensity value shown for each site is the maximum of those predicted for the site assuming a large earthquake on the San Andreas fault and a large earthquake on the Hayward fault. The map suggests that a future earthquake on either of the faults could cause as much damage at some sites distant from the faults as at sites in the immediate zone of potential surface faulting. ("●" indicates recording sites described by Borcherdt (1970); "▲" indicates recording sites occupied since that report (Gibbs and Borcherdt (1974))

Figure 7. Predicted maximum earthquake intensities on a regional scale using the average intensity increments computed for the generalized geologic units (table 1, col. 6), the empirical intensity vs. distance relation (fig. 3), and the generalized geologic map (Lajoie, personal commun., 1974). The empirical relations used for prediction were derived from only the good 1906 intensity data (see text). The predicted value for each map point is the maximum of that predicted for the point assuming a large earthquake on the San Andreas fault and a large earthquake on the Hayward fault. Letters A-E indicate grades of the San Francisco intensity scale (see appendix 1). The map delineates

earthquake problem areas from potential earthquakes on either the San Andreas or Hayward faults and shows that the earthquake hazards are not uniformly distributed throughout the area. For the points closest to the San Andreas fault the map shows more detailed delineations of intensity than did the 1906 intensity maps due to the detailed geologic control currently available and the scarcity of 1906 intensity data available in some areas.

Figure 8. Comparison of earthquake intensity scales. A, Comparison of San Francisco scale and Rossi-Forel scale presented by Wood (1908, p. 226). B, Comparison of Rossi-Forel scale and modified Mercalli scale presented by Wood and Neumann (1931, p. 280-281) and Richter (1958, p. 651).

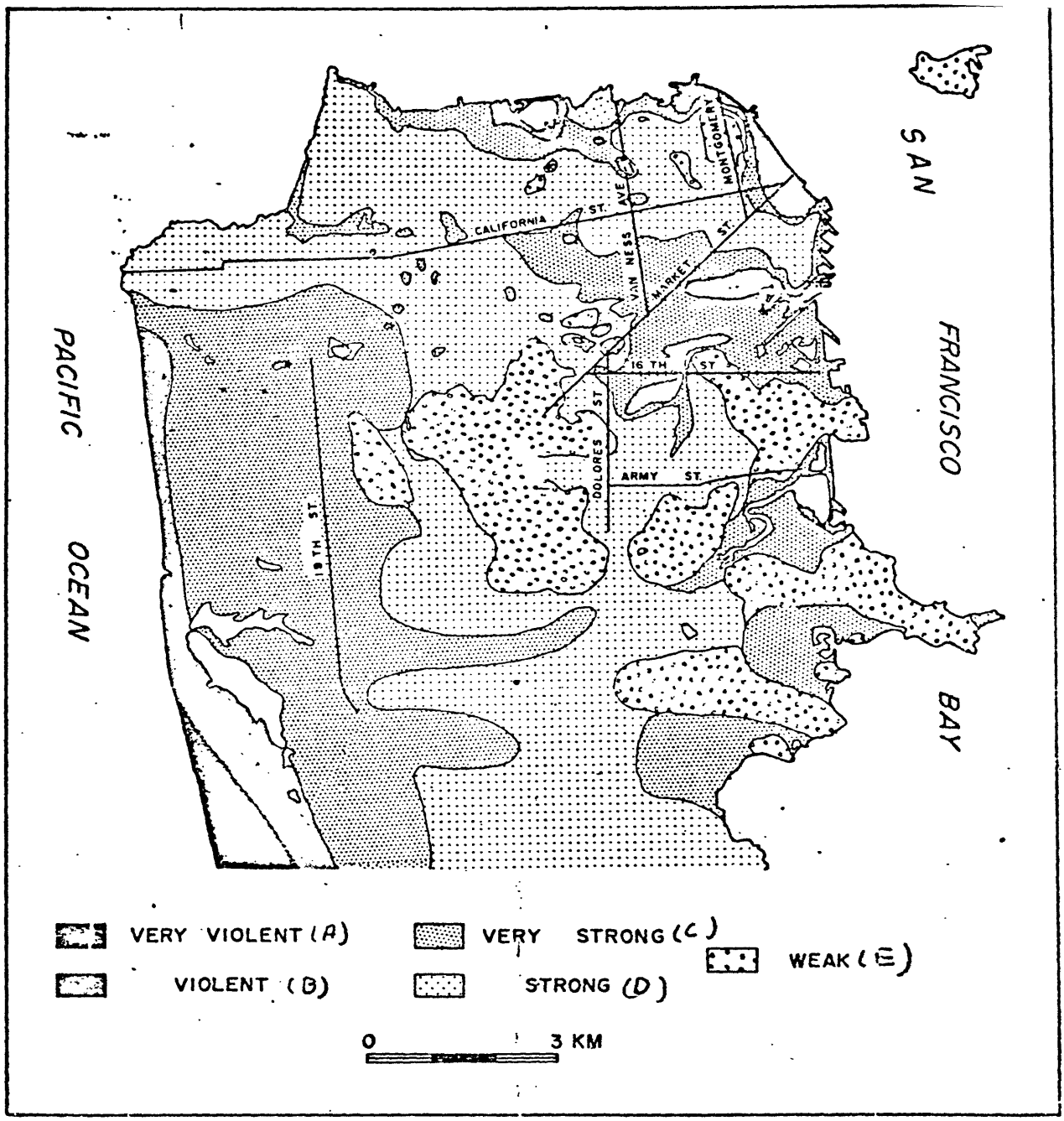
SAN FRANCISCO BAY
PACIFIC OCEAN
CALIFORNIA ST.
VAN NESS AVE.
MARKET ST.
MONTGOMERY ST.
16 TH ST.
DOLORES ST.
ARMY ST.
18 TH ST.
VERY VIOLENT (A)
VIOLENT (B)
VERY STRONG (C)
STRONG (D)
WEAK (E)
0
3 KM

Figure 1

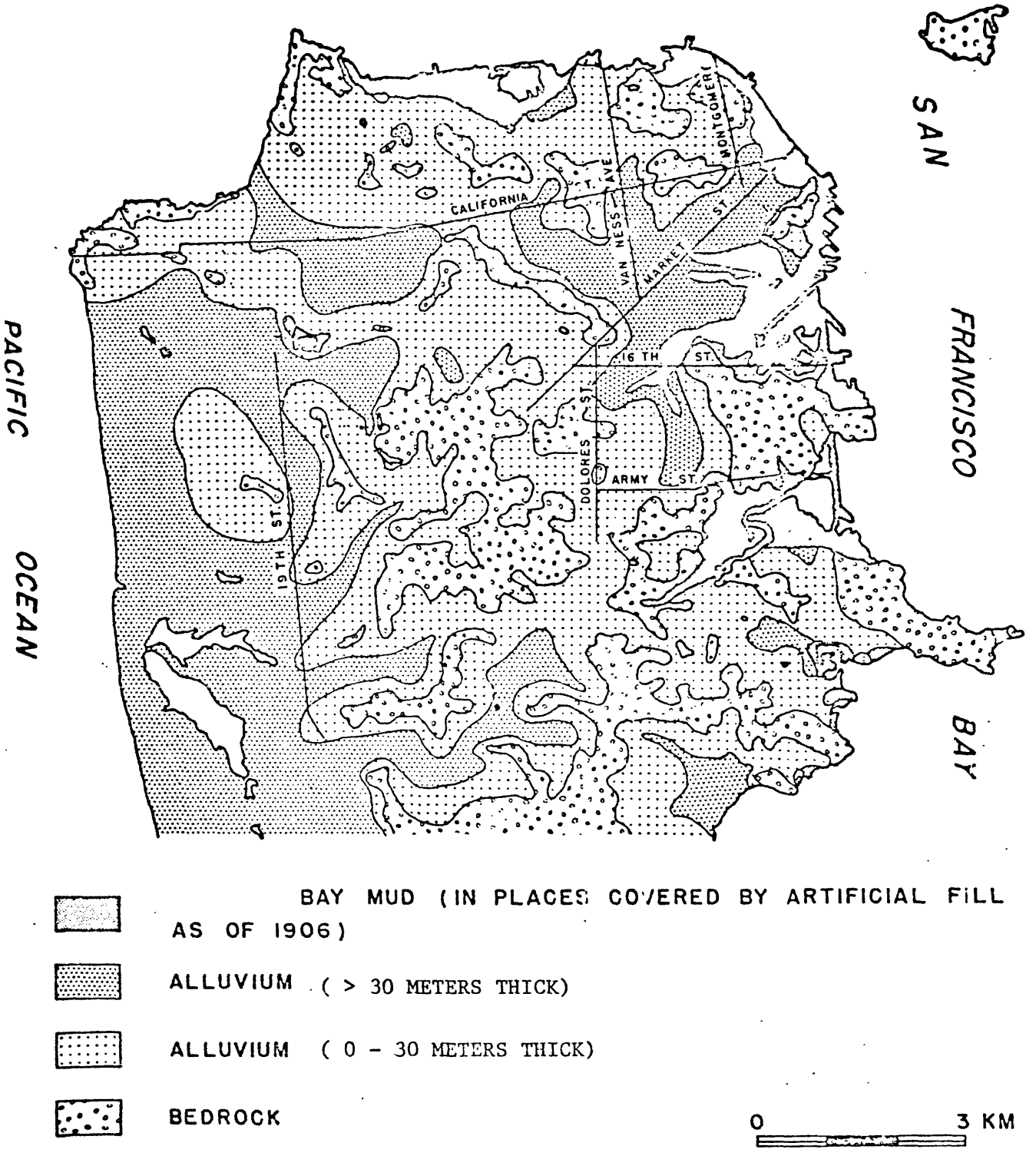
SAN FRANCISCO BAY
PACIFIC OCEAN
CALIFORNIA
VAN NESS AVE
MARKET ST
MONTGOMERY ST
16 TH ST
DOLORES ST
ARMY ST
19TH ST
BAY MUD (IN PLACES COVERED BY ARTIFICIAL FILL AS OF 1906)
ALLUVIUM (> 30 METERS THICK)
ALLUVIUM (0 - 30 METERS THICK)
BEDROCK
0
3 KM

igure 2

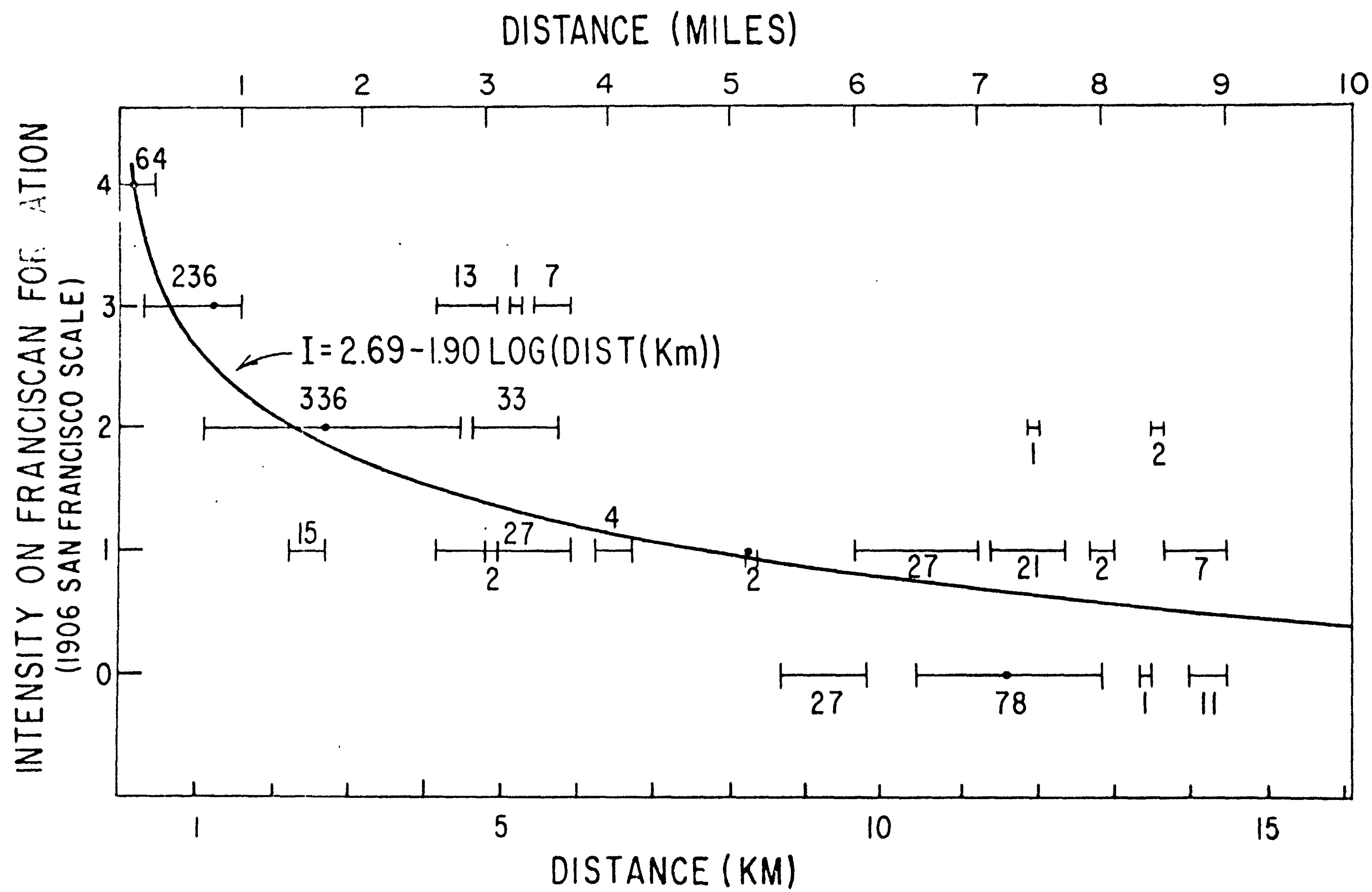
DISTANCE (MILES)
INTENSITY ON FRANCISCAN FOR ATION
(1906 SAN FRANCISCO SCALE)
I=2.69-1.90 LOG(DIST(Km))
64
236
13
1
7
336
33
15
27
2
4
2
27
21
2
7
1
2
27
78
1
11
DISTANCE (KM)

Figure 3

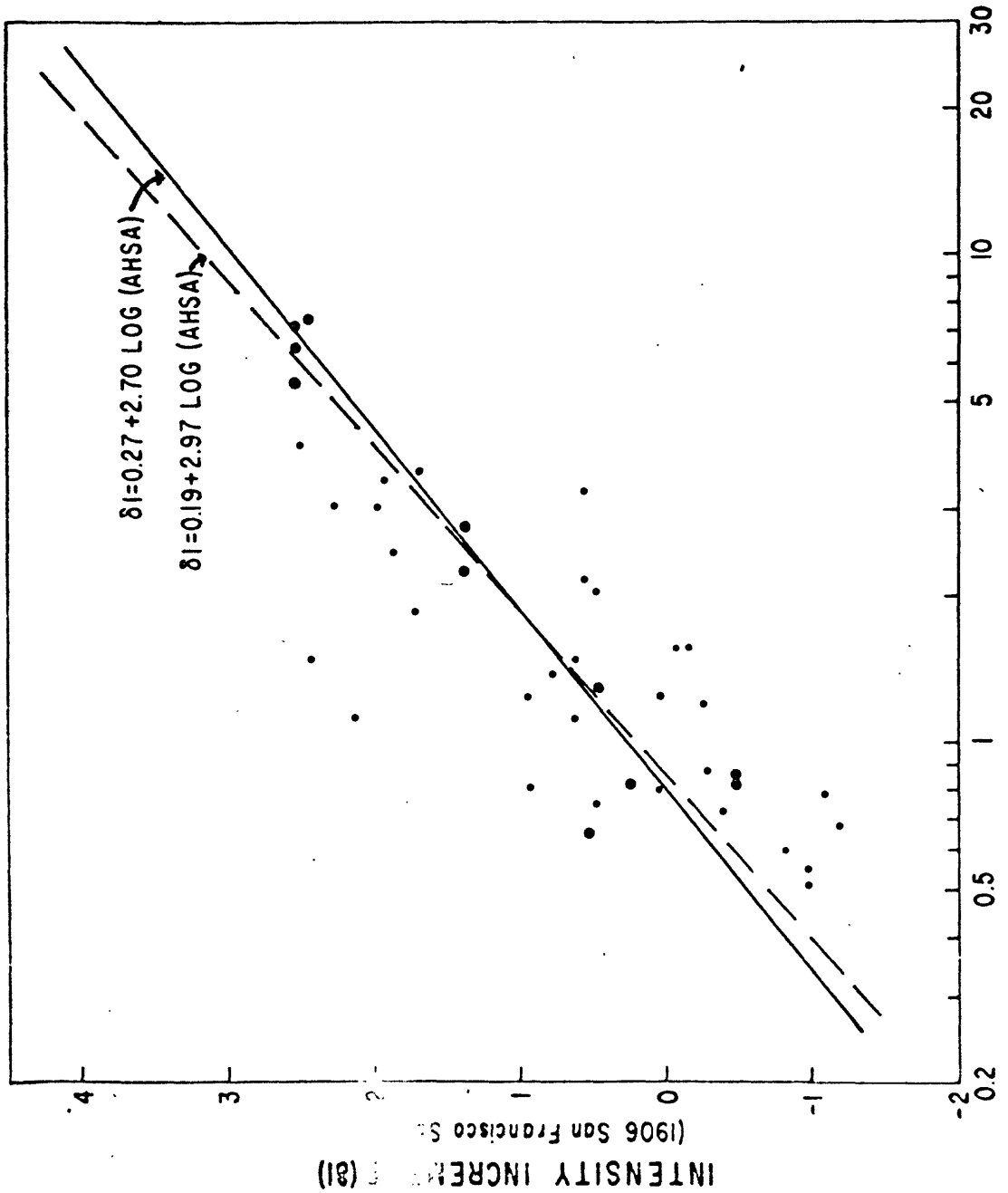
AVERAGE HORIZONTAL SPECTRAL AMPLIFICATION (AHSA)
0.2
0.5
1
5
10
20
30
-2
-1
0
1
2
3
4
81=0.27+2.70 LOG (AHSA)
81=0.19+2.97 LOG (AHSA)
INTENSITY INCREM (81)
(1906 San Francisco S

Figure 4

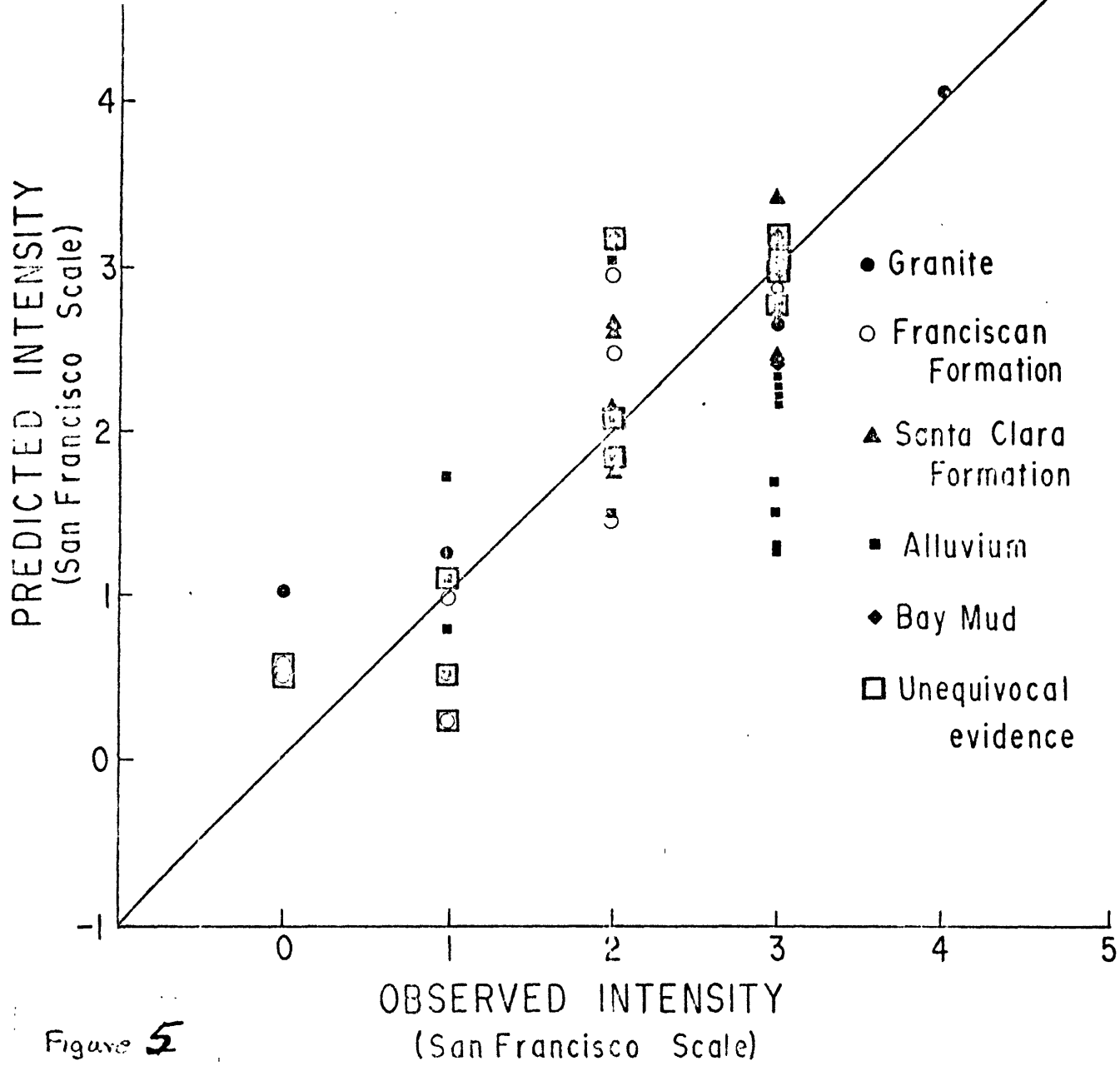
PREDICTED INTENSITY
(San Francisco Scale)
OBSERVED INTENSITY
(San Francisco Scale)
-1
0
1
2
3
4
5
Granite
Franciscan Formation
Santa Clara Formation
Alluvium
Bay Mud
Unequivocal evidence

Figure 5

A

San Francisco scale	Rossi-Forel scale
Grade A	10
Grade B	10
	9
Grade C	8
Grade D	8
	7
Grade E	7

B

Fossi-Forel scale	Modified Mercalli scale
10	X-XII
9+	IX
8+ to 9-	VIII
8-	VII
6 to 7	VI

Figure 8

Table 1

HORIZONTAL AMPLIFICATIONS, INTENSITY INCREMENTS (MEASURED AND PREDICTED) AND INTENSITIES (MEASURED (1906) AND PREDICTED) FOR LOW-STRAIN RECORDING SITES TOGETHER WITH MEANS AND STANDARD DEVIATIONS FOR VARIOUS SAMPLES***

Recording site identification	Distance (km)		Horizontal amplification wrt Franciscan	Intensity increment wrt Franciscan		Earthquake intensities (S.F. scale)		
	San Andreas	Hayward		Measured	Predicted	Hayward Predicted	San Andreas Predicted	San Andreas Observed
			SURFACE LAYER--BEDROCK (granite)					
H16	2.90	32.83	0.60	-0.19	-0.32	-0.51	1.49	2.0
I16	7.89	37.66	0.50	-0.99	-0.53	-0.83	0.45	0.0
H17	4.83	34.92	0.72	-0.39	-0.11	-0.35	1.28	1.0
P17	7.89	37.66	0.55	-0.99	-0.44	-0.74	0.55	0.0
R17	7.08	36.21	0.77	-1.08	-0.04	-0.31	1.04	0.0
Mean			0.63	-0.65	-0.29	- .55	0.96	0.60
Standard deviation			0.11	.55	0.21	.23	.45	.89

Table 1--Continued

HORIZONTAL AMPLIFICATIONS, INTENSITY INCREMENTS (MEASURED AND PREDICTED) AND INTENSITIES (MEASURED (1906) AND PREDICTEI FOR LOW-STRAIN RECORDING SITES TOGETHER WITH MEANS AND STANDARD DEVIATIONS FOR VARIOUS SAMPLES***

Recording site identification	Distance (km)		Horizontal amplification wrt Franciscan	Intensity increment wrt Franciscan		Earthquake intensities (S.F. scale		
	San Andreas	Hayward		Measured	Predicted	Hayward Predicted	San Andreas Predicted	San Andreas Observed
SURFACE LAYER--BEDROCK (Franciscan Formation)								
BLM	0.64	28.00	1.24	-0.05	0.53	0.47	3.58	3.0
GGP	7.24	22.69	0.81	0.94	0.03	0.14	1.08	2.0
J5*	14.65	15.93	0.82	0.52	0.03	0.44	0.51	1.0**
I7	14.65	15.61	0.82	-0.48	0.03	0.46	0.51	0.0**
J7	14.65	15.93	0.65	0.52	-0.23	0.18	0.25	1.0**
I8	14.65	15.61	0.85	-0.48	0.08	0.50	0.56	0.0**
L11	8.21	22.21	0.80	0.05	0.02	0.15	0.97	1.0
K16	4.18	25.43	0.75	0.49	-0.06	-0.04	1.45	2.0
L16	2.41	27.20	1.24	0.04	0.52	0.49	2.48	2.0
Q16	1.77	27.68	1.39	0.78	0.66	0.61	2.87	3.0
T16	1.93	31.70	1.58	-0.15	0.81	0.65	2.95	2.0
Mean				.20	.22	.37	1.56	1.55
Standard deviation				.48	.34	.22	1.19	1.04
K1	21.40	8.69	0.46		-0.63	0.28	-0.46	
S17	31.70	1.77	1.46		0.72	2.94	0.56	
CYH	21.40	8.85	0.50		-0.55	0.34	0.51	
Mean			.96		.14	.54	1.27	
Standard deviation			.36		.45	.72	1.21	

Table 1--Continued

HORIZONTAL AMPLIFICATIONS, INTENSITY INCREMENTS (MEASURED AND PREDICTED) AND INTENSITIES (MEASURED (1906) AND PREDICTED) FOR LOW-STRAIN RECORDING SITES TOGETHER WITH MEANS AND STANDARD DEVIATIONS FOR VARIOUS SAMPLES***

Recording site identification	Distance (km)		Horizontal amplification wrt Franciscan	Intensity increment wrt Franciscan		Earthquake intensities (S.F. scale) Hayward	San Andreas	
	San Andreas	Hayward		Measured	Predicted	Predicted	Predicted	Observed
SURFACE LAYER--BEDROCK (Santa Clara Formation)								
P1	4.83	24.94	1.49	0.61	0.74	0.78	2.14	2.0
P2	4.83	24.94	1.12	0.61	0.40	0.44	1.79	2.0
K9	4.18	23.17	2.09	0.49	1.14	1.24	2.65	2.0
K17	4.51	22.05	2.17	0.55	1.18	1.32	2.63	2.0
L17	0.48	30.26	0.87	-0.29	0.11	-0.01	3.40	3.0
Q17	6.76	21.24	2.48	1.89	1.34	1.51	2.45	3.0
Mean			1.70	.64	.82	.88	2.51	2.33
Standard deviation			.64	.70	.49	.59	.54	.52
SURFACE LAYER--BEDROCK (Page Mill Basalt)								
L3*	5.63	24.14	2.13	0.74	1.16	1.23	2.42	2.0
J4*	6.12	23.66	1.94	1.80	1.05	1.13	2.25	3.0
Mean			2.04	1.27	1.11	1.18	2.34	2.5
Standard deviation			.13	.75	.08	.07	.12	.71

Table 1--Continued

HORIZONTAL AMPLIFICATIONS, INTENSITY INCREMENTS (MEASURED AND PREDICTED) AND INTENSITIES (MEASURED (1906) AND PREDICTED) FOR LOW-STRAIN RECORDING SITES TOGETHER WITH MEANS AND STANDARD DEVIATIONS FOR VARIOUS SAMPLES***

Recording site identification	Distance (km)		Horizontal amplification	Intensity increment wrt Franciscan		Earthquake intensities (S.F. scale) Hayward	San Andreas	
	San Andreas	Hayward	wrt Franciscan	Measured	Predicted	Predicted	Predicted	Observed
SURFACE LAYER--BEDROCK (serpentine and ultramafic rocks)								
H9	2.09	28.00	1.56	-0.08	0.80	0.74	2.88	2.0
J16	0.16	29.61	0.66	-1.19	-0.22	-0.32	3.98	3.0
Mean			1.11	- .64	.29	.21	3.43	2.50
Standard deviation			.64	.78	.72	.75	.78	.71
SURFACE LAYER--BEDROCK (Great Valley Sequence)								
Q13*	31.38	4.35	1.21		0.50	1.98	0.35	
Q14*	32.99	4.83	0.87		0.10	1.50	-0.09	
P19*	36.05	6.12	1.25		0.53	1.73	0.27	
R19*	34.44	5.15	2.44		1.32	2.66	1.09	
T19*	33.96	4.51	1.55		0.79	2.24	0.57	
19B*	5.63	35.89	1.16		0.45	0.19	1.71	
19C*	2.90	32.83	1.63		0.84	0.66	2.66	
19E*	4.99	34.44	1.21		0.50	0.27	1.86	
19W*	7.56	37.34	1.49		0.74	0.45	1.76	
Mean			1.42		.64	1.30	1.13	
Standard deviation			.45		.34	.93	.92	

Table 1--Continued

HORIZONTAL AMPLIFICATIONS, INTENSITY INCREMENTS (MEASURED AND PREDICTED) AND INTENSITIES (MEASURED (1906) AND PREDICTED) FOR LOW-STRAIN RECORDING SITES TOGETHER WITH MEANS AND STANDARD DEVIATIONS FOR VARIOUS SAMPLES***

Recording site identification	Distance (km)		Horizontal amplification wrt Franciscan	Intensity increment wrt Franciscan		Earthquake intensities (S.F. scale) Hayward	San Andreas	
	San Andreas	Hayward		Measured	Predicted	Predicted	Predicted	Observed
SURFACE LAYER--ALLUVIUM (older bay sediments)								
J1*	8.85	20.92	2.37	2.11	1.29	1.47	2.18	3.0
H2*	11.10	18.51	1.56	2.29	0.80	1.08	1.50	3.0
K2	13.20	16.25	1.49	2.44	0.74	1.13	1.30	3.0
Q2	9.17	20.44	1.12	2.14	0.40	0.61	1.27	3.0
T2*	4.51	25.43	1.69	1.55	0.89	0.91	2.34	3.0
H4*	5.95	23.66	2.07	1.78	1.12	1.21	2.34	3.0
K4*	9.33	18.99	1.63	2.15	0.84	1.11	1.69	3.0
K5	12.39	17.86	2.76	1.38	1.46	1.78	2.[illegible]	[illegible]
K7	12.39	17.86	2.23	1.38	1.22	1.53	1.83	2.0[illegible]
R7	14.16	16.09	1.29	0.49	0.57	0.97	1.08	1.0**
H8	10.94	18.67	3.10	2.28	1.60	1.88	2.32	3.0
J8	5.47	24.62	1.86	1.71	1.00	1.05	2.29	3.0
K8	7.56	22.21	3.14	1.98	1.61	1.75	2.64	3.0
L8	7.08	20.60	3.47	1.92	1.73	1.93	2.81	3.0
J11	5.63	24.78	1.20	-0.26	0.49	0.53	1.75	1.0
K11	10.46	20.12	0.82	0.25	0.04	0.26	0.80	1.0
Q11	1.61	28.81	3.60	1.70	1.78	1.70	4.07	4.0
T11	4.51	25.75	3.29	0.55	1.67	1.68	3.12	2.0
L19*	2.74	27.84	2.17	0.14	1.18	1.13	3.04	2.0
Mean				1.47	1.08	1.25	2.13	
Standard deviation				.83	.50	.48	.80	

Table 1--Continued

HORIZONTAL AMPLIFICATIONS, INTENSITY INCREMENTS (MEASURED AND PREDICTED) AND INTENSITIES (MEASURED (1906) AND PREDICTED) FOR LOW-STRAIN RECORDING SITES TOGETHER WITH MEANS AND STANDARD DEVIATIONS FOR VARIOUS SAMPLES***

Recording site identification	Distance (km)		Horizontal amplification wrt Franciscan	Intensity increment wrt Franciscan		Earthquake intensities (S.F. scale) Hayward	San Andreas	
	San Andreas	Hayward		Measured	Predicted	Predicted	Predicted	Observed
SURFACE LAYER--ALLUVIUM (older bay sediments) (continued)								
I4*	24.46	5.79	2.19		1.19	2.43	1.25	
R8*	19.47	7.24	1.18		0.47	1.53	0.71	
T8	14.32	13.68	4.67		2.08	2.61	2.58	
L9	8.85	17.86	3.92		1.87	2.19	2.77	
S12*	17.06	11.59	0.86		0.10	0.77	0.45	
W15*	27.84	2.74	2.07		1.13	2.99	1.08	
I18	13.36	13.52	2.72		1.45	1.99	2.00	
K18	23.17	4.83	3.63		1.78	3.18	1.88	
L18	16.25	10.14	2.32		1.26	2.04	1.65	
P18	18.83	7.56	2.84		1.50	2.52	1.77	
S18	17.06	9.50	3.24		1.65	2.49	2.00	
T18	21.40	4.99	5.03		2.17	3.53	2.33	
Mean			2.44	1.47	1.20	1.68	1.96	2.53
Standard deviation			1.09	.83	.57	.80	.79	.84

Table 1--Continued

HORIZONTAL AMPLIFICATIONS, INTENSITY INCREMENTS (MEASURED AND PREDICTED) AND INTENSITIES (MEASURED (1906) AND PREDICTED) FOR LOW-STRAIN RECORDING SITES TOGETHER WITH MEANS AND STANDARD DEVIATIONS FOR VARIOUS SAMPLES***

Recording site identification	Distance (km)		Horizontal amplification wrt Franciscan	Intensity increment wrt Franciscan		Earthquake intensities (S.F. scale) Hayward	San Andreas	
	San Andreas	Hayward		Measured	Predicted	Predicted	Predicted	Observed
SURFACE LAYER--BAY MUD (younger bay mud)								
P5	14.81	15.45	6.43	2.53	2.46	2.89	2.92	3.0**
Q5	14.97	15.29	7.15	2.54	2.58	3.02	3.04	3.0**
T5*	14.16	16.42	7.50	1.49	2.64	3.02	3.14	2.0
H7	14.32	15.77	4.02	2.50	1.90	2.32	2.40	3.0
P7	14.81	15.45	5.45	2.53	2.26	2.70	2.73	3.0**
T7	13.04	17.54	7.39	2.43	2.62	2.95	3.19	3.0**
Mean				2.34	2.41	2.82	2.90	2.83
Standard deviation				.42	.29	.27	.30	.41
H1	14.48	15.61	4.84		2.12	2.55	2.61	
Q1	11.27	18.67	5.52		2.28	2.55	2.97	
T1	19.96	10.30	3.41		1.71	2.48	1.94	
R2*	10.78	18.83	3.44		1.72	1.99	2.45	
H3*	13.20	16.74	5.75		2.33	2.69	2.89	
K3*	13.84	15.93	5.31		2.23	2.64	2.76	
L4*	13.84	15.77	2.69		1.43	1.85	1.96	
P4*	7.89	21.89	2.88		1.51	1.66	2.50	
Q4	9.66	20.60	5.21		2.21	2.41	3.03	
R4*	18.99	11.43	8.56		2.79	3.47	3.06	
I5A	10.14	20.12	16.25		3.54	3.76	4.32	
I5B	9.66	20.60	13.75		3.35	3.54	4.17	
I5C	8.69	21.57	12.29		3.22	3.38	4.12	
R5	10.46	19.96	9.13		2.87	3.09	3.62	
T9	21.56	6.76	6.75		2.51	3.63	2.67	
I11	14.48	15.61	6.43		2.46	2.88	2.94	
Q12*	26.55	3.06	1.73		0.92	2.69	0.91	

Table 1--Continued

HORIZONTAL AMPLIFICATIONS, INTENSITY INCREMENTS (MEASURED AND PREDICTED) AND INTENSITIES (MEASURED (1906) AND PREDICTED) FOR LOW-STRAIN RECORDING SITES TOGETHER WITH MEANS AND STANDARD DEVIATIONS FOR VARIOUS SAMPLES***

Recording site identification	Distance (km)		Horizontal amplification wrt Franciscan	Intensity increment wrt Franciscan		Earthquake intensities (S.F. scale) Hayward	San Andreas	
	San Andreas	Hayward		Measured	Predicted	Predicted	Predicted	Observed
SURFACE LAYER--BAY MUD (younger bay mud) (continued)								
$L_1$14*	20.28	9.01	3.28		1.67	2.55	1.88	
$L_2$14*	19.96	9.33	5.54		2.28	3.13	2.50	
$L_3$14*	19.63	9.66	2.86		1.50	2.32	1.74	
$L_4$14*	19.31	9.98	3.53		1.75	2.55	2.00	
$L_5$14*	18.99	10.30	3.48		1.74	2.50	2.00	
$L_6$14*	18.67	10.62	2.91		1.52	2.27	1.80	
H15*	22.21	7.56	3.12		1.61	2.63	1.74	
H18*	24.78	5.63	4.19		1.95	3.22	2.00	
Q18	24.62	5.79	2.55		1.37	2.61	1.42	
R18	23.50	6.76	3.74		1.82	2.94	1.91	
Mean			5.67		2.15	2.75	2.59	
Standard deviation			3.31		.61	.49	.79	

*Predicted intensities determined from analog amplifications.

**Observed intensity San Francisco scale. For other sites observed intensity was Rossi Forel Scale which was converted to San Francisco Scale, X ↔ 4.0, IX ↔ 3.0, VIII-IX ↔ 2.0, VII-VIII ↔ 1.0, VI-VII ↔ 0.0, where 4.0 to 0.0 is equivalent to A through E.

***Means and standard deviations are computed for samples including sites with analog amplifications as well as those sites with spectral amplifications. See table 2 for means and standard deviations computed for samples including only those sites with spectral amplifications.

TABLE 2

STATISTICS FOR SAMPLES OF LOW-STRAIN AMPLIFICATIONS AND INTENSITY INCREMENTS WITH RESPECT TO FRANCISCAN FORMATION FOR VARIOUS GEOLOGIC UNITS

Geologic Unit	Average Horizontal Spectral Amplification		Intensity Increment (1906 San Francisco scale)	
	Mean	Standard Deviation	Mean	Standard Deviation
Granite	0.63	0.11	-0.29	0.21
Franciscan Formation	1.00	0.38	0.19	0.47
Great Valley Sequence*	1.42	0.45	0.64	0.34
Santa Clara Formation	1.70	0.64	0.82	0.49
Alluvium	2.44	1.08	1.34	0.58
Bay Mud	7.08	3.78	2.43	0.58

*Amplification determined from analog values as no spectral amplification values were available for this geologic unit (see Gibbs and Borcherdt, 1974 for a comparison of analog and spectral amplifications)